AD_____

Award Number: W81XWH-11-1-0371

TITLE: Intracellular Protein Delivery for Treating Breast Cancer

PRINCIPAL INVESTIGATOR: Dr. Yi Tang

CONTRACTING ORGANIZATION: University of California Los Angeles
Los Angeles, CA 90095

REPORT DATE: August 2014

TYPE OF REPORT: Final

PREPARED FOR: U.S. Army Medical Research and Materiel Command
Fort Detrick, Maryland 21702-5012

REPORT DOCUMENTATION PAGE

Form Approved
OMB No. 0704-0188

1. REPORT DATE	2. REPORT TYPE	3. DATES COVERED
August 2014	Final	15 May 2011 to 14 May 2014

4. TITLE AND SUBTITLE
Intracellular Protein Delivery for Treating Breast Cancer

5a. CONTRACT NUMBER

5b. GRANT NUMBER
W81XWH-11-1-0371

5c. PROGRAM ELEMENT NUMBER

6. AUTHOR(S)
Yi Tang

E-Mail: yitang@ucla.edu

5d. PROJECT NUMBER

5e. TASK NUMBER

5f. WORK UNIT NUMBER

7. PERFORMING ORGANIZATION NAME(S) AND ADDRESS(ES)
University of California Los Angeles
420 Westwood Plaza
Los Angeles, CA 90095

8. PERFORMING ORGANIZATION REPORT NUMBER

9. SPONSORING / MONITORING AGENCY NAME(S) AND ADDRESS(ES)
U.S. Army Medical Research and Materiel Command
Fort Detrick, Maryland 21702-5012

10. SPONSOR/MONITOR'S ACRONYM(S)

11. SPONSOR/MONITOR'S REPORT NUMBER(S)

12. DISTRIBUTION / AVAILABILITY STATEMENT
Approved for Public Release; Distribution Unlimited

13. SUPPLEMENTARY NOTES

14. ABSTRACT
Encapsulating anticancer protein therapeutics in nanocarriers is an attractive option to minimize active drug destruction and increase local accumulation at disease sites. Tumor specific ligands can further facilitate in targeting the nanocarriers to the tumor cells. Rationally designed non-covalent protein nanocapsules, incorporating copper-free "click chemistry" moieties, polyethylene glycol (PEG) units, redox-sensitive crosslinker, and tumor specific targeting ligand, have been synthesized to selectively deliver intracellular protein therapeutics to tumor cells via receptor-mediated endocytosis. These nanocapsules can be conjugated to different targeting ligands of choice, such as anti-Her2 antibody single-chain variable fragment and luteinizing hormone releasing hormone (LHRH) peptide, which result in specific and efficient accumulation within tumor cells overexpressing corresponding receptors. LHRH-conjugated nanocapsules selectively delivered recombinant p53 and its tumor-selective super variant into targeted tumor cells, which led to reactivation of p53-mediated apoptosis. Our results validate a general approach for targeted protein delivery into tumor cells using cellular-responsive nanocarriers.

15. SUBJECT TERMS
Nanogels, core-shell, redox-responsive, apoptosis, breast cancer.

16. SECURITY CLASSIFICATION OF:			17. LIMITATION OF ABSTRACT	18. NUMBER OF PAGES	19a. NAME OF RESPONSIBLE PERSON
a. REPORT	b. ABSTRACT	c. THIS PAGE			USAMRMC
U	U	U	UU	21	19b. TELEPHONE NUMBER *(include area code)*

Table of Contents

INTRODUCTION

Specific induction of cell death in tumors is considered one of the most desired and effective anticancer therapies. Effective strategies to activate the apoptotic pathway, or other death mechanisms, are currently being intensely pursued. A potent chemotherapy option is directly arming the cancer cells with executioner proteins or apoptotic-inducing proteins that are not targeted by anti-apoptotic maneuvers found in many tumors. In this proposal, we will develop a new method to treat breast cancer by using a native-protein delivery approach. This is a platform to deliver proteins in native forms into cells. The key design feature of our strategy is to first encapsulate protein molecules in a thin layer of water soluble, positively charged, degradable polymer to form nanometer-sized nanocapsules. The nanocapsule shell facilitates uptake of the protein content into cells, and protects the protein both during in vivo circulation and endocytosis. To endow the nanocapsules biodegradability once entered the target cells, the polymer shell is crosslinked with redox-sensitive crosslinkers that can be reduced upon encountering the reducing environment of the cytoplasm. Our overall research objective is to thoroughly evaluate this delivery method as a potentially new therapeutic modality for breast cancer treatment. Three aims will be pursued in parallel and results from each aim will be used to guide the refinement of other aims and the overall research objective. 1) Delivering different target proteins to breast cancer cell lines using this approach, including the tumor specific apoptin; 2) Equipping the protein nanocapsules with specific cancer cell targeting ligands; 3) Examining the in vivo potency and pharmacokinetics of the nanocapsules.

BODY

Summary of State of Work

Specific Aim 1: Delivering different target proteins to breast cancer cell lines using protein nanocapsules

Task 1. Preparing and characterizing of Apoptin contained nanocapsules

-COMPLETED

This task has been completed and published in *Nano Today,* **2013, 8,** 11-20. ***(SEE REPORT 1 BELOW)***

We also characterized a new nanocapsule formulation in which eGFP and transcription factor P53 is included. The task has been published in *Journal of the American Chemical Society,* **2014**, 136, 15319-15325. ***(SEE REPORT 2 BELOW)***

Task 2. *in vitro* studying Apoptin contained nanocapsules

-COMPLETED

This task has been completed and published in *Nano Today,* **2013, 8,** 11-20. ***(SEE REPORT 1 BELOW)***

Specific Aim 2: Equipping protein nanocapsules with specific cancer cell targeting ligands;

Task 3. Preparing and testing of MMP activatable cell penetrating peptides (ACCPs)-coupled nanocapsules

-COMPLETED

This task is described here. New chemistry is introduced and new peptide ligands are used, which is published in *Journal of the American Chemical Society*, **2014**, 136, 15319-25. ***(SEE REPORT 2 BELOW)***

Task 4. Preparing and testing of ligand-receptor affinity based targeting: Transferrin (Tf) and Herceptin

-COMPLETED

Completed and described here, published in *Journal of the American Chemical Society*, **2014**, 136, 15319-25. ***(SEE REPORT 2 BELOW)***

Specific Aim 3: Examining the *in vivo* potency and pharmacokinetics of the nanocapsules.

Task 5. Evaluating *in vivo* distribution of protein nanocapsules

-COMPLETED

This task has been partially performed and published in *Nano Today,* **2013, 8,** 11-20.***(SEE REPORT 1 BELOW)***

Task 6. Examining the *in vivo* pharmacokinetics of nanocapsules

-NOT COMPLETED DUE TO INSUFFICIENT TIME

We were not able to complete this aim in time at the completion of this grant. We worked with Institute of Melanoma and Bone Cancer Research (www.imbcr.org) and devised a set of in vivo mice experiments. However, the amount of nanocapsule requirement was too large and we were not able to complete synthesis of the entire batch.

Task 7. Determing the *in vivo* delivery efficacy of nanocapsules

-COMPLETED

This task has been completed and published in *Nano Today,* **2013, 8,** 11-20. ***(SEE REPORT 1 BELOW)***

The work on apoptin and p53 nanocapsules described here published in Zhao et al, *Nano Today,* **2013, 8,** 11-20 **and in** *Journal of the American Chemical Society*, **2014**, **136,** 15319-25. **Both manuscripts are reformatted here.**

REPORT 1. Degradable Polymeric Nanocapsule for Efficient Intracellular Delivery of a High Molecular Weight Tumor-Selective Protein Complex (Tasks 1, 2, 5, and 7)

1.1 Introduction

The most desirable anticancer therapy is both potent and specific towards tumor cells(Atkins and Gershell, 2002; Gibbs, 2000). Many conventional small molecule chemotherapeutics do not discriminate between cancerous and normal cells, cause damage to healthy tissues, and are therefore unable to be administered at high dosage. In contrast, cytoplasmic and nuclear proteins that selectively alter the signaling pathways in tumor cells, reactivate apoptosis and restore tissue homeostasis, can delay tumor progression with less collateral damage to other tissues(Reed, 2003; Russo et al., 2006). Using stimuli-responsive nanocarriers for the intracellular delivery of such proteins, including human tumor suppressors (Brown et al., 2009)and exogenous tumor-killing proteins (Backendorf et al., 2008; Los et al., 2009; Noteborn, 2009), is attractive as a new anti-cancer therapy modality.

Apoptin is a 121-residue protein derived from chicken anemia virus (Backendorf et al., 2008). When transgenically expressed, apoptin can induce p53-independent apoptosis in a variety of tumor and transformed cells(Zhuang et al., 1995), while leaving normal and untransformed cells unaffected(DanenVanOorschot et al., 1997). Apoptin exists as a globular multimeric complex, composed of thirty to forty subunits, with no well-defined secondary structure (Leliveld et al., 2003). While the exact mechanism of the tumor selectivity is unresolved, apoptin is known to translocate to the nucleus where tumor-specific phosphorylation at residue Thr108 takes place, leading to accumulation of apoptin in nucleus and activation of the apoptotic cascade in tumor cell(Danen-van Oorschot et al., 2003). In normal cells, apoptin is not phosphorylated at Thr108 and is located mostly in the cytoplasm, where it aggregates and undergoes degradation (Rohn et al., 2002). Because of the high potency in inducing this exquisite tumor-selective apoptosis, apoptin has been investigated widely as an anti-tumor therapeutic option (Backendorf et al., 2008). Different gene therapy approaches have been used to administer apoptin to mouse xenograft tumor models, in which significant reduction in tumor sizes and prolonged lifespan of mice have been observed without compromising the overall health (Peng et al., 2007; Pietersen et al., 1999; van der Eb et al., 2002). However, as with other gain-of-function therapy candidates, *in vivo* gene delivery approaches using viral vectors may lead to unwanted genetic modifications and elicit safety concerns(Edelstein et al., 2007). While protein transduction domain (PTD)-fused apoptin has been delivered to cells(Sun et al., 2009; Tavassoli et al., 2004), this approach suffers from inefficient release of the cargo from endosomes and instability of the unprotected protein (Murriel and Dowdy, 2006). Development of nanoparticle carriers to aid the functional delivery of apoptin to tumor cells is therefore desirable (Shi et al., 2010).

We chose to work with recombinant maltose-binding-protein fused apoptin (MBP-APO) that can be solubly expressed from *Escherichia coli*, whereas native apoptin forms inclusion bodies(Leliveld et al., 2003). MBP-APO has been shown to similarly assemble into a multimeric protein complex, which exhibits the essential functions and selectivity of native apoptin(Leliveld et al., 2003). Nanoparticle-mediated delivery of functional MBP-APO poses unique challenges (Gu et al., 2011). First, MBP-APO preassembles into large complex with an average diameter of ~40 nm and molecular weight of ~2.4 MDa (Leliveld et al., 2003). To achieve nanocarrier sizes that are optimal for *in vivo* administration (~100 nm) (Adiseshaiah et al., 2010), a loading strategy that forms compact particles is desirable. Second, in order to maintain the multimeric state of functional MBP-APO, the protein loading and releasing steps need to take place under very mild, physiological conditions in the absence of surfactants. Lastly, the nanocarrier must completely disassemble inside the cell to release the MBP-APO in its native and unobstructed form to ensure the correct spatial presentation of key residues within the apoptin portion, including the nuclear localization/export signals, the phosphorylation site and other elements important for downstream signaling.

In the current study, we selected a polymeric nanocapsule (NC) strategy for the functional delivery of MBP-APO, in which the protein complex is noncovalently protected in a water soluble polymer shell (Figure 1). This slightly positively-charged shell shields the MBP-APO from serum proteases and surrounding environment, while enabling cellular uptake of the polymer-protein complex through endocytosis (Gu et al., 2009). The polymeric layer is weaved together by redox-responsive cross-linkers containing disulfide bond (S-S) that can be degraded once the NCs are exposed to the reducing environment in cytoplasm (Zhao et al., 2011). No covalent bonds are formed between the protein cargo and the polymer shell, which ensures complete disassembly of the capsule layer and release of native MBO-APO inside the cell. Using this approach, we show that MBP-APO can be efficiently delivered to induce apoptosis in cancer cell lines selectively both *in vitro* and *in vivo*.

1. 2 RESULTS AND DISCUSSION

1.2.1. Synthesis and characterization of apoptin nanocapsules

MBP-APO (pI = 6.5) was first purified from *E. coli* extract using an amylose-affinity column. Dynamic Light Scattering (DLS) measurement revealed an average hydrodynamic radius of 36.1 nm, consistent with the reported size for the recombinant MBP-APO complex (Leliveld et al., 2003). Transmission Electron Microscopy (TEM) analysis of MBP-APO showed similarly sized protein complexes (Figure 1c and enlarged in Figure 1d). Interestingly, MBP-APO complexes appear to adopt a disk-shaped structure despite the lack of defined secondary structure from the apoptin component. Since the apoptin portion of the protein can self-assemble into the ~40-mer complex, we propose a three dimensional arrangement of MBP-APO in which the C-terminal apoptin forms the central spoke of the wheel-like structure (Figure 1b), with the larger MBP portion distributes around the apoptin. The planar arrangement allows the apoptin portion of the fusion protein to remain accessible to its protein partners, which may explain how the MBP-APO fusion retains essentially all of the observed functions of native apoptin.

The reversible encapsulation strategy for producing apoptin NCs is shown in Figure 1a. Following electrostatic deposition of the monomers acrylamide (**1** in Figure 1a) and *N*-(3-aminopropyl)methacrylamide (**2**), and the cross-linker *N*,*N*'-bis(acryloyl)cystamine (**3**), at a molar ratio of 1.5:1:0.14, onto MBP-APO (1 mg) in carbonate buffer (5 mM, pH 9.0), *in situ* polymerization was initiated with the addition of free radical initiators and proceeded for one hour. The molar ratio and the time of reaction reported were optimized to minimize protein aggregation and precipitation, as well as to maximize the solution stability of the resulting NCs (designated below as S-S APO NC). Excess monomers and cross-linkers were removed using ultrafiltration and S-S APO NC was stored in PBS buffer (pH 7.4). DLS clearly showed increase in average diameter of the sample to ~75 nm with a slightly positive ζ-potential value of 2.8 mV. TEM analysis of the S-S APO NC confirmed the nearly doubling in diameter of the spherical particle (Figure 1e). Unexpectedly, the NCs displayed dark contrast upon uranyl acetate staining, which hints that the cores of the particles were very densely packed. As expected from the incorporation of redox-responsive cross-linker **3**, the reduction of NCs size can be seen upon treatment of the reducing agent glutathione (GSH) (2 mM, 6 hours, 37°C). As shown in Figure 1f, the densely packed NCs were completely dissociated into ~30 nm particles, confirming the reversible nature of the encapsulation process. As a control, we also synthesized nondegradable MBP-APO NCs (ND

APO NC) using *N*,*N*'-methylene bisacrylamide as the cross-linker with same monomer and protein concentrations under identical reaction conditions. Whereas similarly sized NCs were formed, no degradation of ND APO NC can be observed in the presence of GSH.

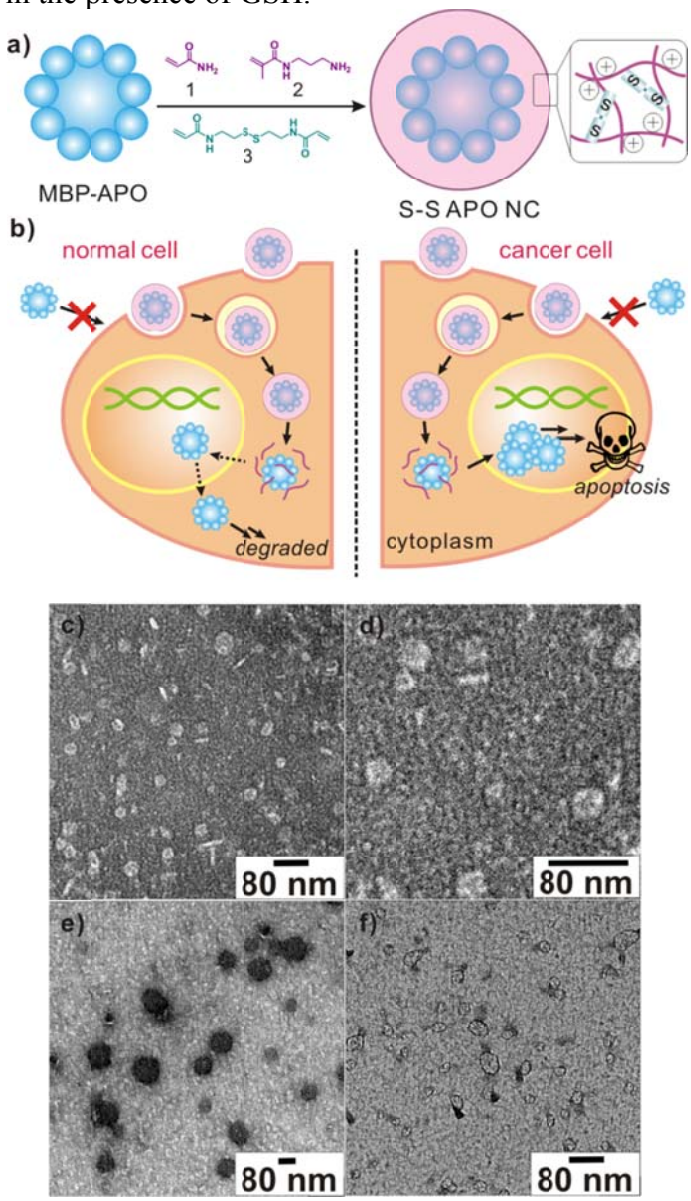

Figure 1. Degradable nanocapsules for apoptin delivery. a-b) Schematic diagram of synthesis of degradable apoptin nanocapsules (S-S APO NC) and delivery into tumor cells to induce apoptosis; TEM images of c) native MBP-APO; d) enlarged image of MBP-APO; e) S-S APO NC; and f) degraded S-S APO NC after treatment with 2 mM GSH for 6 hours at 37°C;

1.2.2. Cellular uptake and localization of nanocapsules

We next examined the cellular uptake of the S-S APO NC and cellular localization of the cargo. If the unique tumor selectivity of MBP-APO is maintained following the encapsulation and release processes, we expect the delivered MBP-APO to either accumulate in the nuclei of the tumor cells, or to localize in the cytoplasm of noncancerous cells. Prior to the polymerization process, the MBP-APO protein was conjugated to amine-reactive rhodamine (Rho-APO). Subsequent encapsulation yielded similarly sized NCs as unlabeled S-S APO NCs. Fluorescent microscopy showed all NCs readily penetrated the cell membrane and are present in the cytoplasm of MDA-MB-231 cells within one hour. When the relative amounts of positively-charged monomer **2** were reduced in the NC shell, corresponding decreases in ζ potentials of the NCs were measured by DLS, which led to decreases in cellular internalization. The cellular trafficking of the internalized S-S Rho-APO NCs in HeLa cells was investigated for 2 hours by monitoring colocalization using fluorescent markers for early and

late endosomes (Figure 2a). Colocalization of Rho-APO with early endosomes was detected at the highest levels after 30 minutes and decreased at later time points. In contrast, colocalization of Rho-APO with late endosome remained low throughout the trafficking studies. Colocalization of Rho-APO with nuclei became evident after 2 hours, indicating endosomal escape and nuclear entry of the released apoptin protein. These results suggested that S-S Rho-APO NCs were trafficked into early endosomes upon internalization and at least a significant portion of the internalized NCs and the cargo can escape from the endosomal compartment.

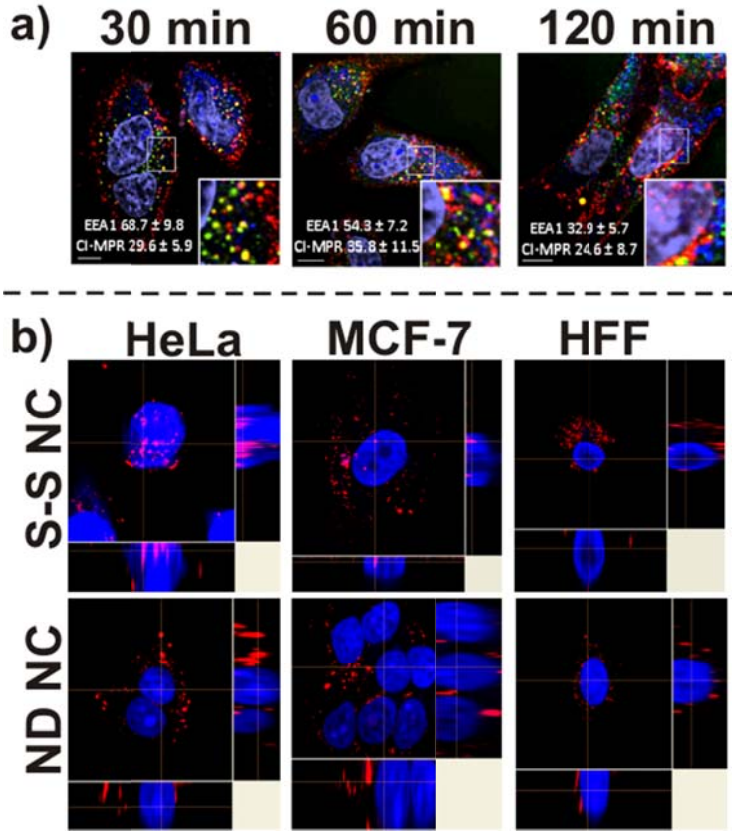

Figure 2. Protein nanocapsule cellular trafficking and localization. a) The trafficking of Rho-APO in S-S NCs through endosomes. HeLa cells were incubated with 20 nM S-S Rho-APO NCs (red) at 37°C for various time periods, 30, 60 and 120 min. Early endosomes were detected by early endosome antigen 1 (EEA1, green). Late endosomes were detected by cation-independent mannose-6-phosphate receptor (CI-MPR, blue). Nuclei were stained with DAPI and shown as purple. The scale bar represents 10 μm. The percentage of fluorescence colocalization was quantified by calculating colocalization coefficients using Manders' overlap coefficient (>10 samples) and shown in each figure; b) confocal microscopy of cellular localization of Rho-APO encapsulated in S-S NC and ND NC to cancer cell lines HeLa and MCF-7, and noncancerous HFF. Nuclei were stained with DAPI (blue). The scale bar is 20 μm.

To analyze protein localization using confocal microscopy, two cancer cell lines HeLa and MCF-7, together with the noncancerous human foreskin fibroblast (HFF), were treated with either S-S Rho-APO NC or ND Rho-APO NC (Figure 2b). In the case of ND Rho-APO NCs, red fluorescence signals remained in the cytoplasm for all three cell lines, indicating the encapsulated Rho-APO proteins were well-shielded by the nondegradable polymer shell and the internal nuclear localization sequences were not accessible to the transport machinery. In stark contrast, when HeLa cells were treated with S-S Rho-APO NC, strong red fluorescence of rhodamine was present in the nuclei, resulting in intense pink color as a result of overlapping of rhodamine and DAPI fluorescence. Z-stacking analysis confirmed the Rho-APO to be localized inside of the nuclei. Similar results were observed with MCF-7 cells, although the fluorescence intensity was not as strong as in the HeLa cells. These results confirmed that the Rho-APO delivered can indeed be released in native forms inside the cytoplasm and enter the nuclei. More importantly, the tumor-specificity of delivered apoptin proteins towards cancer cell lines were demonstrated in the confocal analysis of noncancerous HFF cells treated with S-S Rho-APO NC, as all of the dye signals remained in the cytoplasm and no nuclear accumulation was observed.

1.2.3. Tumor-selective cytotoxicity of apoptin nanocapsules

We then investigated whether the MBP-APO protein delivered still possesses its function to induce tumor-selective apoptosis. The potency and selectivity of S-S APO NC were tested on various cell lines including HeLa, MCF-7, MDA-MB-231, and HFF (Figure 3a-d). MTS assay was used to measure cell viability 48 hours after addition of the protein and NC. For each cell line, ND APO NC and native MBP-APO were used as negative controls. When S-S APO NC was added to a final concentration of 200 nM, all three cancer cell lines had no viable cells, whereas ~75 % of the HFF had survived. The IC_{50} values were 80 and 30 nM for HeLa and MDA-MB-231, respectively. The IC_{50} for MCF-7 was higher at ~110 nM, which may be due to the deficiency in the terminal executioner caspase 3 and reliance on other effector caspases for apoptosis(Burek et al., 2006). As expected, native MBP-APO and ND APO NC did not significantly decrease the viability of any cell lines tested, consistent with the inability to enter cells and release MBP-APO in cytoplasm, respectively. The IC_{50} values of S-S APO NC towards MDA-MB-231 increased as the surface charge of the NC became more neutral, suggesting more efficient internalization can improve S-S NCs cytotoxicity. The morphologies of MDA-MB-231 and HFF cells were examined under various treatments. Only the S-S APO NC treated MDA-MB-231 cells exhibited blebbing and shrinkage, which are hallmarks of apoptotic cell death (Figure 3e). Using TUNEL assay, S-S APO NC treated MDA-MB-231 also showed nuclear fragmentation associated with apoptosis, whereas cells treated with native MBP-APO and ND APO NC at the same concentratio, as well as HFF treated with 200 nM S-S APO NC (Figure 3e), had no sign of apoptosis. Collectively, these results demonstrated that the recombinant MBP-APO delivered by the degradable NCs retains the potency and selectivity as the transgenically expressed apoptin in previous studies (Backendorf et al., 2008).

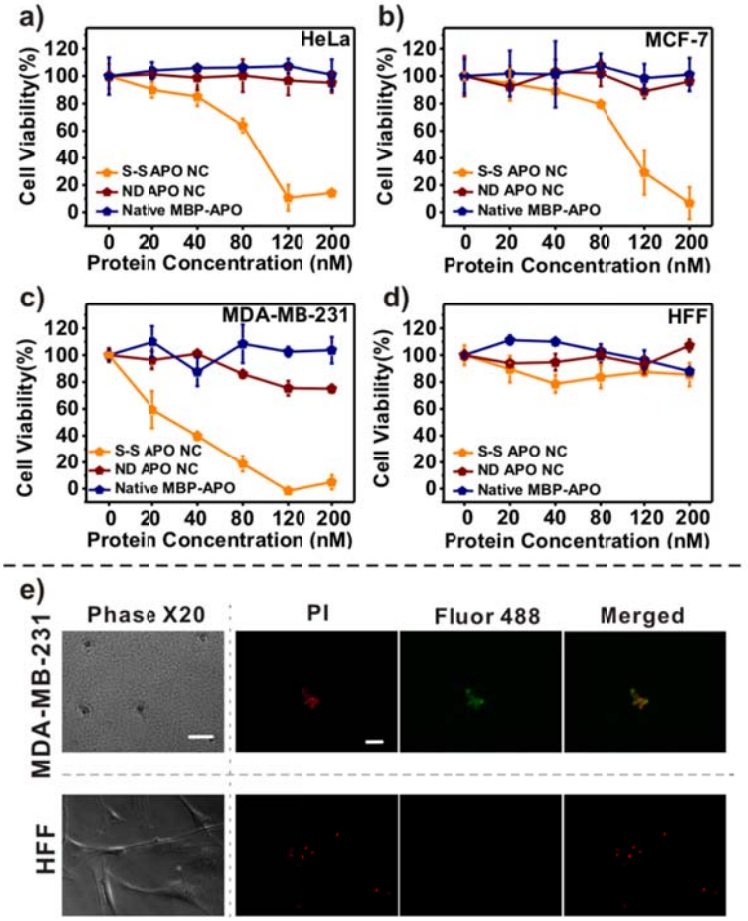

Figure 3. Cytotoxicity and apoptosis observed following nanocapsule delivery. (a) HeLa; (b) MCF-7; (c) MDA-MB-231; or (d) HFF cells with treatment of different concentrations of S-S APO NC, ND APO NC, and native MBP-APO. (e) Apoptosis induced by S-S APO NC determined by TUNEL assay. Images on the left are bright field microscopy images of MDA-MB-231 and HFF cells treated for 24 hours with 200 nM S-S APO NC. The scale bar represents 50 µm. Images right of the dash line shows detection of apoptotic fragmentation of the nucleosome after same treatment using APO-BrdU™ TUNEL assay kit. The scale bar represents 50 µm. Red fluorescence represents the propidium-iodide (PI)-stained total DNA, and green fluorescence represents the Alexa Fluor 488-stained nick end label, the indicator of apoptotic DNA fragmentation. The merged pictures combine the PI-stained nuclei and the Alexa Fluor 488-stained nick end label. (Note

the bright field images do not overlap with the fluorescent microscopy images; cells were detached and collected for TUNEL assay after treatment).

1.2.4. In vivo evaluation of apoptin nanocapsules

We further examined the potency of S-S APO NC in a mouse xenograft model. Female athymic nude (*nu/nu*) mice were subcutaneously grafted on the back flank with 5×10^6 MCF-7 breast cancer cells. When the tumor volume reached 100-200 mm^3 (day 0), mice were randomly separated into different groups and treated with intratumoral injection of PBS, MBP-APO, S-S APO NC. In addition, S-S NC with bovine serum albumin (S-S BSA NC) was added as a nonlethal protein cargo control to test the effects of the S-S NC polymer component on tumor cells *in vivo*. Tumors treated with saline, S-S BSA NC or native MBP-APO expanded rapidly and reached the maximum limit (>2500 mm^3) within 12 days. In sharp contrast, tumor growth was significantly delayed when treated with S-S APO NC (Figure 4a). Fixed tumor tissues collected from each treatment group was examined for DNA fragmentation using *in situ* TUNEL assay. The images revealed the highest level of cell apoptosis for the tumor harvested from mice treated with S-S APO NC, correlating well with the significantly delayed tumor growth observed for this treatment group and confirming that tumor growth inhibition was indeed due to apoptin-mediated apoptosis (Figure 4b). Collectively, the xenograft study verified that the degradable NCs effectively delivered MBP-APO proteins to tumor cells *in vivo*, which was highly effective in limiting tumor progression. Upon further optimization of the pharmacokinetics of the S-S APO NC, including surface derivatization with active targeting ligands, these particles may be intravenously administered as an anticancer therapy (Kamaly et al., 2012).

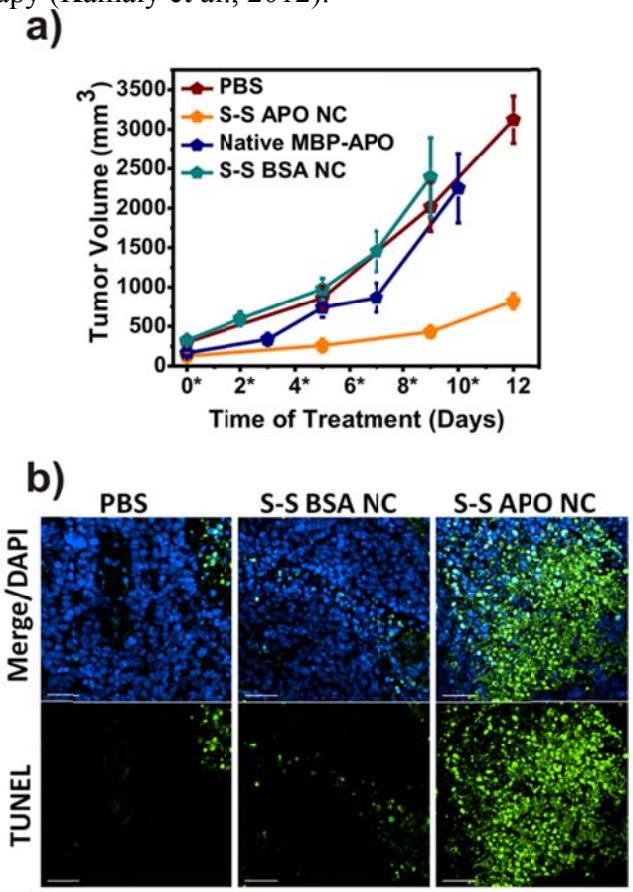

Figure 4. Treatment of apoptin nanocapsules resulted in tumor growth retardation. a) Significant tumor inhibition was observed in the mice treated by S-S APO NC. Female athymic nude mice were subcutaneously grafted with MCF-7 cells and treated with intratumoral injection of MBP-APO (n=4) or S-S APO NC (n=4) (200 μg/mouse) every other day. PBS (n=3) and S-S BSA NC (n=4) were included as negative controls. The average tumor volumes were plotted vs. time. Asterisks indicate injection days. b) Detection of apoptosis in tumor tissues after treatment with different NCs. Cross-sections of MCF-7 tumors were stained with fluorescein-dUTP (green) for apoptosis and DAPI for nucleus (blue). The scale bars represent 50 μm.

REPORT 2. Clickable Protein Nanocapsules for Targeted Delivery of Recombinant p53 Protein. (Tasks 1, 3 and 4)

2.1 Introduction

Virtually all human cancer cells have elaborate anti-apoptotic strategies to overcome apoptosis, which is a vital cellular mechanism to obstruct tumor progression.(Cotter, 2009) The most commonly mutated gene in tumor cells is the tumor suppressor gene *TP53*, the protein product of which promotes apoptosis of aberrant cells through both transcription-dependent and independent mechanisms.(Coles et al., 1992) In this manner, the genome guardian p53 is critically important in eliminating possible neoplastic cells incurred during DNA damage. About 50% of all the human tumors have mutant p53 proteins.(Lacroix et al., 2006) Therefore, restoring p53 function can be a highly effective option for cancer treatment. While functional copies of p53 can resurrect the apoptotic circuitry, it also sensitize the tumor cells towards other various treatments (radio- and chemotherapy).(Blagosklonny, 2002) Different strategies pursuing this goal have been intensively investigated, including small molecules, peptides that overcome p53 mutations and adenovirus/p53 gene delivery vectors.(Friedler et al., 2002; Issaeva et al., 2004; Senzer et al., 2007; Vassilev et al., 2004) While restoring p53 functions in cancer cells has been a tantalizing approach towards combating cancer, the lack of effective delivery method has undermined its potential as an anti-cancer therapeutic.

One critical limitation of previous protein-containing nanocapsule is that the polymer layer is synthesized from a positively charged monomer that enables nonselective entry across cellular membrane. However, since the level of p53 is tightly regulated in normal cell lines, targeted delivery of p53 using functionalized nanocapsules that restricts entry to only cancer cell lines is highly desirable. Hence, new nanocapsule encapsulation strategy that allows facile modification of the polymeric carrier is needed.

To equip the nanocapsules with cancer-targeting ligands such as peptides and antibodies that can enable receptor mediated endocytosis, the surface of the nanocapsules must be decorated with reactive handles that facilitate aqueous-based conjugation chemistry. The chemistry utilized must be nondenaturing and maintaining the native form of protein cargo. This is especially important for p53 delivery since the protein forms a tetrameric complex that is prone to aggregation and loss of function.(Bell et al., 2002b) The reaction must also be orthogonal to the nanocapsule synthesis chemistry and compatible with the designed degradation mechanism of the polymer capsule, such as disulfide mediated redox-sensitive degradation. One of the most versatile reactions that are compatible with a protein-based cargo is the copper-free click chemistry that utilizes azides and aryl cyclooctynes.(Baskin et al., 2007; Mbua et al., 2011; Ning et al., 2008) Click chemistry has been used for modification of nanoparticles for directed conjugation of ligands and chromophores.(Koo et al., 2012; Welser et al., 2009) In this report, we demonstrate that pegylated protein nanocapsules containing reactive azido groups on the surface can be synthesized, which allows facile conjugation to various tumor-targeting ligands. More importantly, we show that recombinant p53 can be selectively delivered to specific cancer cell lines using nanocapsules clicked with targeting ligands.

2.2 RESULTS AND DISCUSSION

2.2.1. Synthesis of nanocapsules with clickable monomer

Our synthesis strategy for protein nanocapsules is shown in Figure 1. Monomers and redox-sensitive crosslinkers are polymerized *in situ* around the target protein to form a noncovalent shell that encapsulates the protein. The monomer acrylamide (**1**) is used as a general building block of the water-soluble shell. The nanocapsules are crosslinked with *N,N'*-bis(acryloyl)cystamine (**3**), which is designed to degrade under high reducing conditions such as the cytosol,(Meister and Tate, 1976) thereby releasing the protein cargo intracellularly. To synthesize a near-neutral polymer shell that does not enter cells via positive charges, we first eliminated the use of positively charged monomers employed in previous designs, such as *N*-(3-aminopropyl)methacrylamide. Instead, we chose *N*-(azidoethyl-decaethylene glycol)-acrylamide (**2**) as the second monomer (Figure 1a). The neutral **2** contains a terminal azido group that can be used as the reactive site for cross-coupling via copper-free click reaction. The ten ethylene glycol unit serves as a water soluble spacer at the surface of the nanocapsules, and provides flexibility to the conjugated targeting ligand. Through copolymerization of **1** and **2**, the azido functionalities can be displayed on the surface of the nanocapsules for

subsequent modification. Monomer **2** was readily prepared by reacting *O*-(2-aminoethyl)-*O'*-(2-azidoethyl)nonaethylene glycol with acryloyl chloride.(Welser et al., 2009) After purification and MS characterization of monomer **2**, we performed the *in situ* polymerization process using green fluorescent protein (GFP) as the cargo. Following one hour of polymerization during which the mole fraction of **2** was kept at 1.5% of total monomers, uniformly sized nanoparticles were synthesized, with an electrostatic potential of ~ -0.9 mV, and an average size of 9.1±0.8 nm.

To verify the presence of azido groups on the surface of the nanocapsules, we performed the copper-free reaction between dibenzylcyclooctyne TAMRA (DBCO TAMRA, **4**) and the GFP nanocapsules prepared from monomers **1** and **2.** As a control, nanocapsules synthesized from **1** alone were also mixed with **4**. After overnight stirring at 4°C, the reaction was subjected to repeated dialysis and ultrafiltration (30K MWCO) to remove any unreacted **4**. The conjugation of TAMRA to the protein nanocapsules were detected by fluorescence emission scan (Figure 1b). Whereas nanocapsules synthesized with both **1** and **2** exhibited the characterized emission peak at 580 nm of TAMRA, the control sample with only **1** showed nearly no signal at the same wavelength. We previously established that most of the nanocapsules prepared via the polymerization method contain a single copy GFP,(Yan et al., 2010) which is also likely here given the nanocapsule synthesized using the new monomers are nearly identical in size. Hence, the number of TAMRA molecules conjugated per nanocapsules was approximated through the comparison of relative intensities of GFP and TAMRA fluorescent intensity. At the chosen 1.5% monomer **2** mole fraction, we approximated that each nanocapsule was conjugated with four TAMRA molecules through the click reaction with accessible azido functional groups.

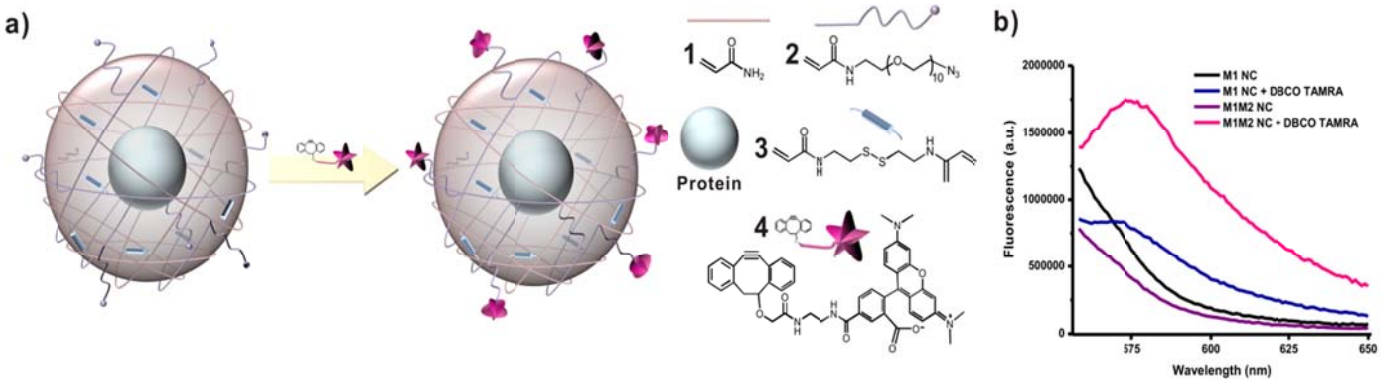

Figure 1. Clickable nanocapsules. **a**) Schematic diagram of clickable, redox-sensitive protein nanocapsules, and scheme of conjugated to DBCO TAMRA using copper-free click chemistry. **b**) Fluorescence spectra of NC samples before and after copper-free click conjugation with DBCO TAMRA.

2.2.2. *Conjugation of nanoparticles with ligands*

After confirming the successful "clicking" of cyclooctyne moieties onto the surface of azido-functionalized nanocapsules, we then developed methods to conjugate cancer targeting ligands. We first selected the luteinizing hormone releasing hormone (LHRH) peptide **5** (Glp-His-Trp-Ser-Tyr-D-Lys-Leu-Arg-Pro-NHEt, Figure 2a), which binds to LHRH receptors that are overexpressed in various hormonal related cancers, such as breast and prostate cancers.(Nagy and Schally, 2005) LHRH receptors are not expressed detectably in most visceral organs and have been targeted in the delivery of small molecules.(Dharap et al., 2003; Dharap et al., 2005) The bifunctional dibenzocyclooctyne-PEG4-N-hydroxysuccinimidyl ester (DBCO-PEG4-NHS ester, **6**) was chosen as the tether (Figure 2a). The peptide **5** was first conjugated to the NHS terminus of **6** through the internal D-Lys designed to serve as a site for coupling. The adduct **7** was verified by LC-MS and purified by HPLC to homogeneity. Subsequently, **7** was added to the azido-functionalized GFP nanoparticles at a molar ratio of 15:1 and allowed to react overnight at 4°C. Following the click reaction, unreacted **7** was removed through ultrafiltration (30K MWCO) and the nanoparticles were dialyzed into phosphate saline buffer. To test the LHRH receptor mediated endocytosis of nanocapsules, we added the LHRH functionalized nanocapsules to the MDA-MB-231 cell line, which is known to overexpress the receptor.(Harris et al., 1991) As controls we also added GFP nanocapsules that are i) positively charged that are

expected to be internalized (monomers **1** and *N*-(3-aminopropyl)methacrylamide) ; ii) azido-functionalized but not conjugated to LHRH (monomers **1** and **2)**; and iii) do not contain azido groups (monomer **1** only). After overnight incubation, the internalization of nanocapsules was visualized by fluorescent microscopy.

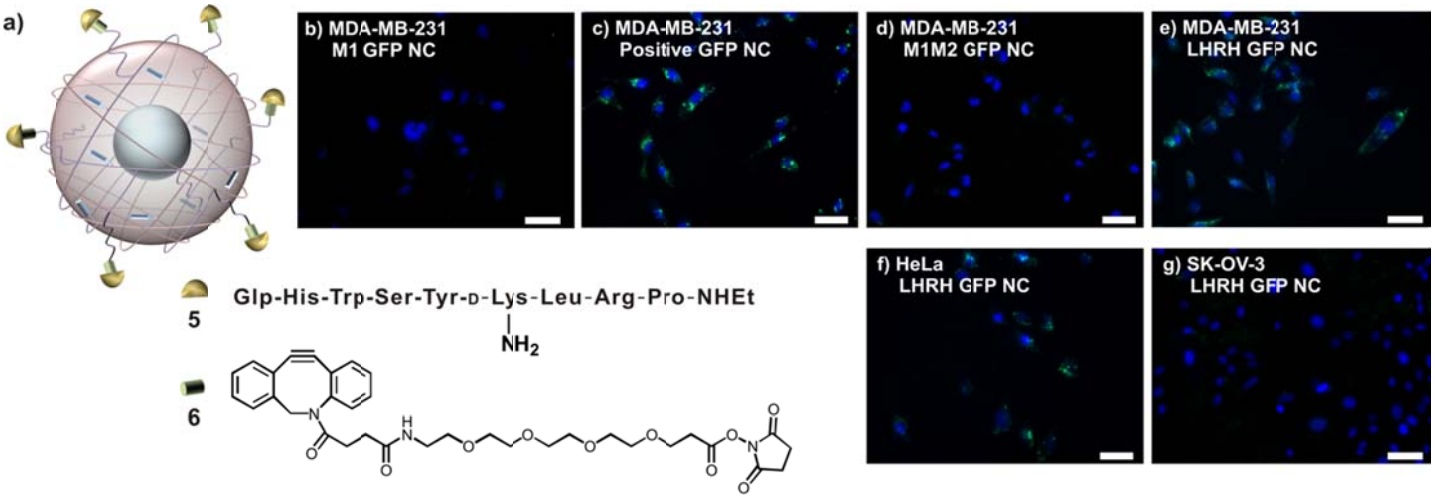

Figure 2. Selective internalization of LHRH conjugated nanocapsules. **a**) Scheme of LHRH S-S NC. Glp is cyclized glutamine; Fluorescent microscopy images of cell lines treated with 400 nM GFP-containing nanocapsules. **b**) MDA-MB-231 treated with GFP nanocapsule synthesized with monomer **1** alone; **c**) MDA-MB-231 treated with positively charged GFP nanocapsule; **d**) MDA-MB-231 treated with GFP nanocapsules synthesized from monomers **1** and **2** (no targeting ligand); **e**) MDA-MB-231 treated with GFP nanocapsules synthesized from monomers **1** and **2** and conjugated with the LHRH targeting ligand); **f**) HeLa cells treated with nanocapsules in **e; g**) SK-OV-3 cells treated with nanocapsules in **e**. Nuclei were stained with DAPI. The scale bars represent 50 μm.

As can be seen from Figure 2b, the positively charged nanocapsules were well-internalized as expected. In contrast, the neutral nanocapsules, either with or without azido groups, were completely not internalized into cells. LHRH-functionalized GFP nanocapsules, however, were efficiently internalized as can be seen from the GFP fluorescence in the cytosol. To quantify the LHRH-receptor mediated endocytosis, FACS was performed on the samples as shown in Figure 3a. The level of internalization through LHRH receptor mediated endocytosis is ~70% level of that observed with positively charged nanocapsules. More importantly, azido-functionalized nanoparticles without LHRH conjugation did not exhibit noticeable internalization compared to no treatment or native GFP controls. Particle trafficking experiments were performed for the LHRH-targeted GFP particles (Figure 3bc). Localization in the early endosomes was observed within 30 minutes, while release into the cytosol was detected at one and two hours after delivery. No significant localization of GFP in the late endosome was observed. To further test the cell selectivity of the protein delivery, we added the LHRH-functionalized NC to various cell lines with varying levels of LHRH receptor expression. When added to cervical cancer cell line HeLa cells that have comparable levels of expression, the amount of internalization were similar to that of MDA-MB-231(Figure 2f). No internalization was seen with the SK-OV-3, which is a LHRH receptor-negative ovarian cancer cell line (Figure 2g).(Dharap and Minko, 2003)

To demonstrate the versatility of the surface functionalization, we conjugated the single-chain variable fragment of the anti-Her2 antibody to the azido-functionalized GFP nanocapsules (antibody to protein nanocapsule molar ratio of 10:1). A maleimide containing bifunctional linker was used to conjugate to cysteine residue on the recombinant scFv (linker to antibody molar ratio of 5:1) (Figure 4). When administered to various cell lines, internalization of GFP nanocapsules was only observed in SK-BR-3 that overexpresses the HER2 receptor, and no fluorescence was seen in triple negative breast cancer cell line MDA-MB-231, HeLa or human foreskin fibroblasts (HFF) (Figure 4). Collectively these data illustrate the polymerization, conjugation and internalization steps are all effective as designed.

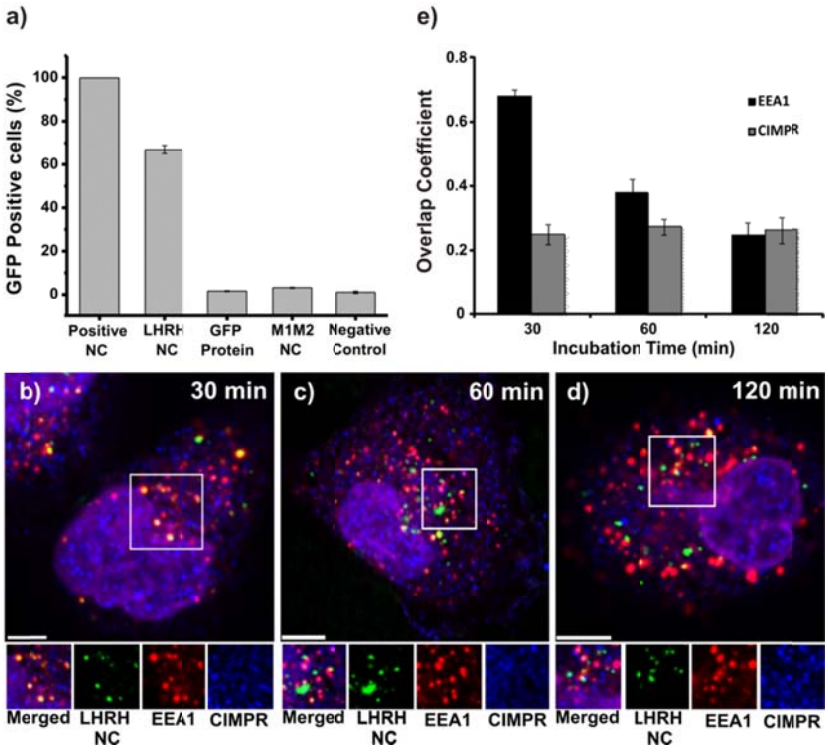

Figure 3. Cellular uptake and trafficking of LHRH nanocapsules by MDA-MB-231 cells. **a**) Different extent of the cellular internalization of 400 nM GFP protein or nanocapsules by MDA-MB-231 cells at 37°C for 12 hours. The mean fluorescence intensity was measured by flow cytometry and was represented as the percentage of fluorescence from MDA-MB-231 cells incubated with positively charged nanocapsules. **b-d**) The trafficking of LHRH-conjugated GFP nanocapsules through endosomes. MDA-MB-231 cells were incubated with 800 nM nanocapsules at 37°C for various time periods, 30, 60 and 120 min. Early endosomes were detected by early endosome antigen 1 (EEA1, green). Late endosomes were detected by cation-independent mannose-6-phosphate receptor (CI-MPR, blue). Nuclei were stained with DAPI and shown as purple. The scale bar represents 10 μm. **e**) Quantification of LHRH-conjugated GFP nanocapsules colocalized with EEA1or CI-MPR endosomes at various incubation times. Colocalization coefficients were calculated using Manders' overlap coefficient (>10 samples). The error bars indicate standard deviation.

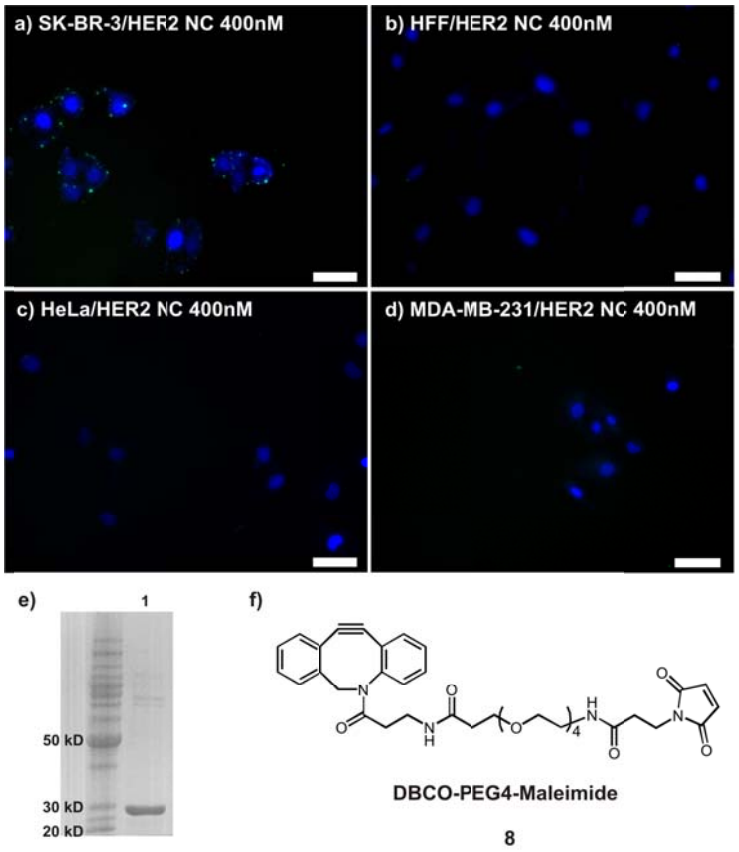

Figure 4. Internalization of HER2 NC. Fluorescent microscopy images of a) SK-BR-3 cells; b) HFF cells; c) HeLa cells; d) MDA-MB-231 cells incubated overnight with 400 nM HER2 NC containing GFP protein. Nuclei were stained with DAPI. The scale bars represent 50 μm. e) SDS-page of purified single-chain variable fragment of anti-HER2 antibody (lane 1). f) Structure of DBCO-PEG4-Maleimide.

2.2.3. *Synthesis of clickable p53 nanocapsules*

We then applied the nanocapsule synthetic steps towards the targeted delivery of p53 to cancer cells. Delivery of recombinant p53 poses significant challenges as the tetrameric complex can readily aggregate and lose activity under non-native condition.(Bell et al., 2002a) The three-dimensional structure of p53 is also not well resolved, and has been shown to be loosely organized, especially in the absence of DNA.(Bell et al., 2002b) Recombinant p53 was expressed from *Escherichia coli*, purified from inclusion bodies and refolded as soluble protein (Figure 5a).(Bell et al., 2002a) The *in situ* polymerization process using monomers **1** and **2**, as well as crosslinker **3** was optimized to minimize aggregation and precipitation of the soluble p53. A final molar fraction of 1.5% of **2** was used in the monomers, while 5% **3** was added as crosslinkers. We found that p53 concentration must be kept at below 0.7 mg/mL and all steps must be performed in sodium bicarbonate containing buffer to avoid aggregation and precipitation (see Materials and Methods). After encapsulation, the azido-functionalized nanocapsules (S-S p53 NC) were buffer-exchanged and concentrated in PBS buffer. Successful encapsulation was monitored by both DLS and TEM as shown in Figure 5b and Figure 5c, respectively. The native p53 tetramer exhibited hydrodynamic diameter of 7.7±0.5 nm, in line with cryo-EM characterizations.(Okorokov et al., 2006; Tidow et al., 2007) Upon encapsulation the average diameter increased to ~27.5±1.0 nm with a ξ-potential of -0.6mV, and the structural uniformity was observed by Transmission Electron Microscopy (TEM). As a non-degradable control, p53-containing nanocapsules crosslinked with the *N*,*N*'-methylene bisacrylamide was also prepared. The physical properties of the azido-functionalized non-degradable p53 nanocapsules (ND p53 NC) were nearly identical to that of the S-S p53 NCs. To examine the encapsulation effectiveness and redox-sensitive release of the p53 nanocapsules, we performed time-dependent ELISA analysis of p53 nanocapsules both in the presence and absence of the reducing agent DTT (Figure 5d). Encapsulated p53 is physically shielded by the polymer layer and is thus unable to be recognized by the anti-p53 antibody. As expected in the absence of DTT, no native p53 in the solution can be

detected within the one hour assay period, indicating the robustness of the polymer layer in both shielding and retaining the p53 cargo. In contrast, the S-S p53 NCs released p53 when 2 mM DTT was added to the nanocapsules, indicating degradation of the crosslinker and release of p53 into the solution. The ND p53 NCs control did not release detectable p53 in the presence of 2 mM DTT, further confirming the redox-responsiveness of the S-S p53 NCs.

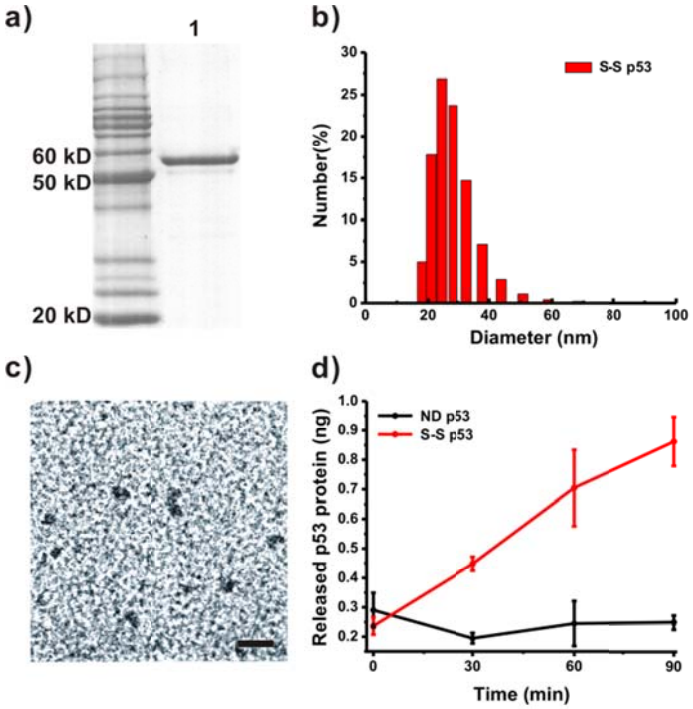

Figure 5. Preparation of recombinant p53 and characterization of LHRH-conjugated p53 nanocapsules. a) SDS-PAGE of refolded p53 protein. b) The hydrodynamic size distribution of S-S p53 NC as measured by DLS. c) TEM image of S-S p53 NC. The scale bar represents 50 nm. d) ELISA assay measuring p53 released from S-S p53 NC and ND p53 NC after treatment with 2 mM DTT over 90 min at 37°C (n=2).

2.2.4. *Internalization and Release of p53 in cancer cells*

To examine the internalization of S-S p53 NCs into cancer cells, we first conjugated the recombinant p53 to rhodamine dye to form Rho-p53. Following encapsulation with 1, 2 and 3 to form rhodamine-labeled NCs, the LHRH peptide 5 was conjugated to the surface using the bifunctional linker 6. When added to MDA-MB-231 cell lines, rhodamine fluorescence can be seen inside the cells after a 12 hour incubation period. When analyzed with confocal microscopy, we observed accumulation of Rho-p53 in the nucleus of the targeted cells, which is the expected localization for the transcription factor (Figure 6b). In contrast, no nuclear overlap between DAPI and rhodamine fluorescence can be observed when the Rho-p53 was encapsulated in nondegradable linker and internalized. This is consistent with the inability of Rho-p53 to escape the polymer shell in the absence of the redox-responsive crosslinker 3. In this case, all the rhodamine signals remained in the cytoplasm (Figure 6a).

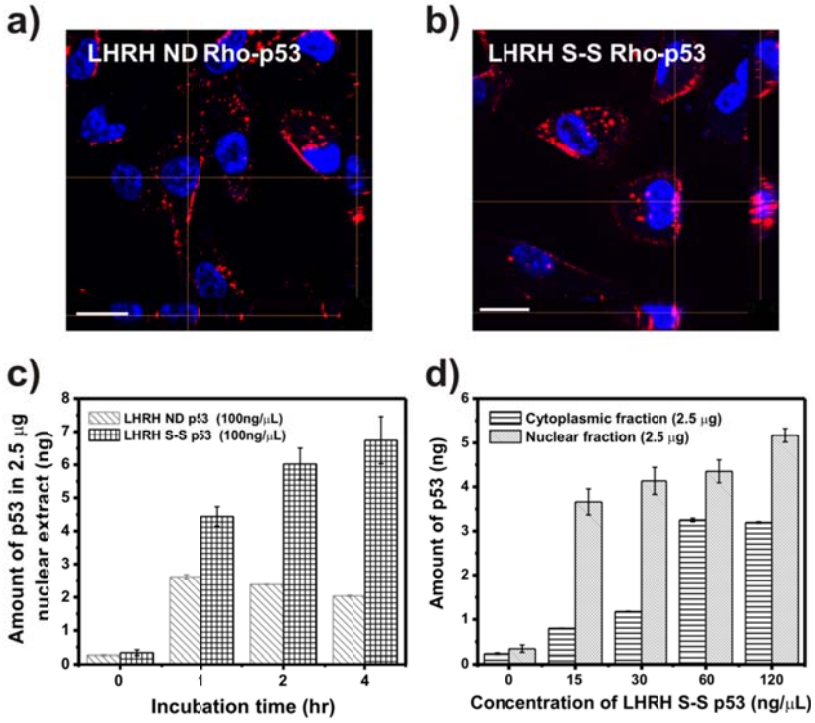

Figure 6. Internalization and location of p53 delivered by designed nanocapsules. Confocal images of MDA-MB-231 cells incubated with 200nM **a**) LHRH-conjugated ND Rho-p53 NC; **b**) LHRH-conjugated S-S Rho-p53 NC; The scale bar represents 20 nm. **c**) ELISA detection of p53 in the nuclear fraction from MDA-MB-231 cells treated with 100 ng/μL LHRH-conjugated ND p53 NC or LHRH-conjugated S-S p53 NC for increasing periods of time; **d**) ELISA detection of p53 in the cytoplasmic and nuclear fraction from MDA-MB-231 cells treated with increasing concentration of LHRH-conjugated S-S p53 NC for one hour.

To further quantify the nuclear localization of delivered p53, we performed the time course ELISA analysis of p53 concentration in nuclear and cytoplasmic fractions of MDA-MB-231 cells treated with 100 ng/μL of S-S p53 NC or ND p53 NC functionalized with LHRH peptide (Figure 6c). The standard curve relating ELISA signal and p53 levels was established using purified recombinant p53. Untreated cells displayed a low level of endogenous p53 (R280K mutant in MDA-MB-231) that is less than 0.5 ng per 2.5 mg of nuclear extract. As shown in Figure 6c, S-S p53 NC treated samples showed a clear accumulation of p53 in the nuclei at time points tested. Close to 7 ng of p53 per 2.5 mg of nuclear extract was observed after four hours. As expected from Rho-p53 localization studies above, significantly higher amounts of p53 can be detected in S-S samples comparing to nondegradable samples. While the ND p53 NC-treated sample showed ~2 ng of nuclei p53 after one hour treatment, no increase was observed after prolonged incubation time. The effect of S-S p53 NC dosage on intracellular p53 concentration was also measured using ELISA. Increasing amount of delivered p53 (from 15 to 120 ng/L) led to increases in both cytosolic and nuclear concentration of p53 after one hour (Figure 6d). Therefore, we have shown that LHRH-functionalized, redox- sensitive nanocapsules can effectively deliver recombinant p53 into cancer cells. The delivered and released p53 can dramatically increase the concentration of p53 in both cytosol and nuclear. The accumulation in nuclei of cancer cells is especially important, as this is the desired site of action for p53 for cancer cell fate reversal.

2.2.5. *Cytotoxicity of p53 Nanocapsules*

To examine the effect of delivered p53 on cell viability, we performed cytotoxicity studies using the LHRH-functionalized nanocapsules. Two different p53 versions were used in this study, the wild type and the tumor selective "super" p53 variant. The super p53 is the gain of function point mutant S121F that has been shown to display more potent apoptotic activity.(Saller et al., 1999) The mutation alters the specificity of p53 binding targets, and in particular, attenuates the activation of MDM2 transcription associated with normal p53 overexpression.(Saller et al., 1999) The decreased MDM2 feedback control therefore increases apoptosis

induction. The 121F mutant kills tumor cells irrespective of p53 status but not wild-type mouse embryo fibroblasts.(Saller et al., 1999) S-S S121F NCs were prepared in the same manner as S-S p53 NC and conjugated to LHRH peptides using click chemistry. Physical characterizations were performed to verify that the NCs were nearly identical in properties. Both LHRH-conjugated p53 NCs were then added to different cancer cell lines and the cytotoxicity was measured using MTS assay after 48 hours. As shown in Figure 7, LHRH-conjugated S-S p53 NCs showed high selectivity towards MDA-MB-231 that overexpresses the LHRH receptor. Nearly no toxicity was observed towards either SK-OV-3 or HFF at 800 nM, the highest concentration assayed. The S121F containing NCs showed potent cytotoxicity, with IC_{50} at ~ 100 nM. In contrast, IC_{50} for the wild type p53 NCs was ~300 nM. We confirmed observed cell death after delivery of S121F is indeed via apoptosis by using TUNEL assay. Negative controls were performed to ensure the observed toxicity is due to the combination of targeted delivery of p53 or tumor selective variant, including i) azido-functionalized S-S S121F NCs not conjugated to LHRH; ii) LHRH conjugated S-S GFP NCs; and iii) azido-functionalized GFP NCs not conjugated to LHRH. In all these controls, the cells remain unaffected by the addition of nanocapsules. These results therefore unequivocally confirm the targeted and functional delivery of p53 can be achieved using the encapsulation and conjugation strategies.

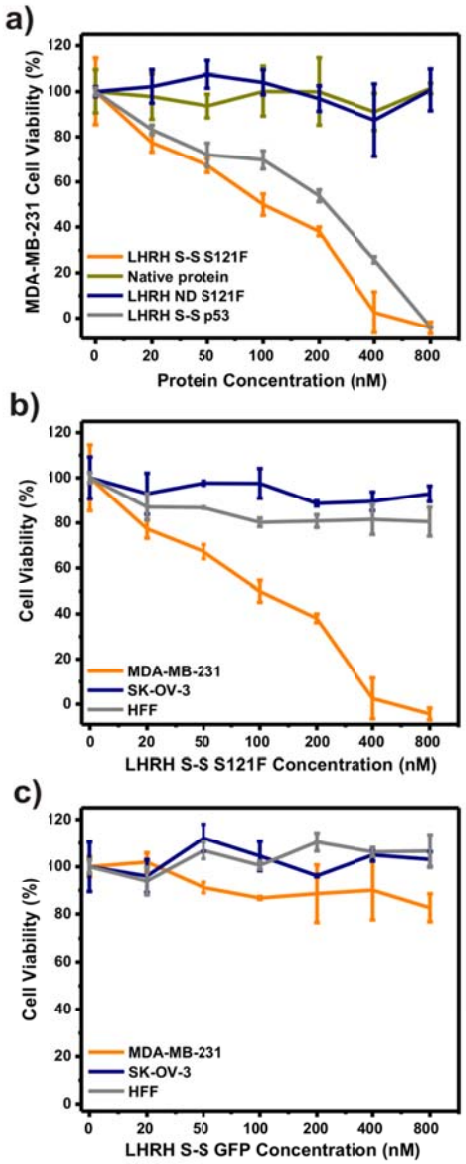

Figure 7. Cytotoxicity of LHRH-conjugated nanocapsules towards tumor cell lines. **a**) MDA-MB-231 cell viability treated with LHRH-conjugated S-S S121F NC, native S121F protein, LHRH-conjugated ND S121F NC, and LHRH-

conjugated S-S p53 NC; **b**) MDA-MB-231, SK-OV-3 and HFF cell lines treated with LHRH-conjugated S-S S121F NC; **c**) MDA-MB-231, SK-OV-3 and HFF cell lines treated with LHRH-conjugated S-S GFP NC.

KEY RESEARCH ACCOMPLISHMENTS

- We synthesized degradable, sub-100 nm, core-shell protein nanocapsules containing the 2.4 MDa apoptin complexes. Recombinant apoptin is reversibly encapsulated in a positively charged, water soluble polymer shell and is released in native form in response to reducing conditions such as the cytoplasm.

- Intracellularly released apoptin induced tumor-specific apoptosis in several cancer cell lines and inhibited tumor growth *in vivo*.

- A new conjugation method of a targeting peptide to the surface of nanocapsules is developed.

- We synthesized polymer nanocapsules for delivery of the cellular guardian transcription factor p53

- Incorporating copper-free "click chemistry" moieties, polyethylene glycol (PEG) units, redox-sensitive crosslinker, and tumor specific targeting ligand in the new design, nanocapsules can selectively deliver intracellular protein therapeutics to tumor cells via receptor-mediated endocytosis.

REPORTABLE OUTCOMES

Publications*:*

1. Muxun Zhao, Biliang Hu, Zhen Gu, Kye-Il Joo, Pin Wang* and Yi Tang* "Degradable Polymeric Nanocapsule for Efficient Intracellular Delivery of a High Molecular Weight Tumor-Selective Protein Complex" 2013, *Nano Today*, 8, 11-20

2. Muxun Zhao, Yarong Liu, Renee S. Hsieh, Nova Wang, Kye-Il Joo, Pin Wang, Zhen Gu, Yi Tang* "Clickable Protein Nanocapsules for Targeted Delivery of Recombinant p53 Protein" 2014, *Journal of the American Chemical Society*, 136, 15319-15325

Presentations in this period:

The following oral presentation was made at American Institute of Chemical Engineers Annual Meeting (**2013**) San Francisco

"Delivery of tumor killing protein to cancer cells." Muxun Zhao, Biliang Hu, Pin Wang, Yi Tang. University of California, Los Angeles, Los Angeles, CA; University of Southern California, Los Angeles, CA

CONCLUSION

We were able to deliver the high molecular weight complex of the tumor-selective MBP-APO using a redox-responsive polymeric NC *in vitro* and *in vivo*. The choice and design of the sub-100 nm NC is well-suited for diverse protein targets because of its mild preparation conditions, reversible encapsulation, efficient membrane penetration, and cytoplasmic release of the protein cargo. We also developed a new polymerization strategy for the synthesis of protein nanocapsules that display azido functional groups on the surface. By using a cyclooctyne and NHS ester or maleimide containing bifunctional linkers, different targeting ligands such as the LHRH peptide and HER2 ScFv can be attached to the surface of the protein nanocapsules. Using GFP as cargo,

we demonstrated the specific internalization of the nanocapsules into cells overexpressing corresponding receptors. Finally, we demonstrated this approach can achieve the functional delivery of the genome guardian p53 protein to trigger apoptosis in targeted cancer cell lines. LHRH-conjugated nanocapsule can be used as a protein delivery system for the treatment of LHRH receptor overexpressing tumor cells. Our results validate a general approach for targeted protein delivery into tumor cells in a cellular-responsive manner, opening up new opportunity for the development of protein anticancer treatment.

REFERENCES

Adiseshaiah, P.P., Hall, J.B., and McNeil, S.E. (2010). Nanomaterial standards for efficacy and toxicity assessment. Wires Nanomed Nanobi *2*, 99-112.

Atkins, J.H., and Gershell, L.J. (2002). Selective anticancer drugs. Nat Rev Drug Discov *1*, 491-492.

Backendorf, C., Visser, A.E., de Boer, A.G., Zliumerman, R., Visser, M., Voskamp, P., Zhang, Y.H., and Noteborn, M. (2008). Apoptin: Therapeutic potential of an early sensor of carcinogenic transformation. Annu Rev Pharmacol *48*, 143-169.

Baskin, J.M., Prescher, J.A., Laughlin, S.T., Agard, N.J., Chang, P.V., Miller, I.A., Lo, A., Codelli, J.A., and Bertozzi, C.R. (2007). Copper-free click chemistry for dynamic in vivo imaging. Proc Natl Acad Sci U S A *104*, 16793-16797.

Bell, S., Hansen, S., and Buchner, J. (2002a). Refolding and structural characterization of the human p53 tumor suppressor protein. Biophys Chem *96*, 243-257.

Bell, S., Klein, C., Muller, L., Hansen, S., and Buchner, J. (2002b). p53 contains large unstructured regions in its native state. J Mol Biol *322*, 917-927.

Blagosklonny, M.V. (2002). P53: An ubiquitous target of anticancer drugs. Int J Cancer *98*, 161-166.

Brown, C.J., Lain, S., Verma, C.S., Fersht, A.R., and Lane, D.P. (2009). Awakening guardian angels: drugging the p53 pathway. Nat Rev Cancer *9*, 862-873.

Burek, M., Maddika, S., Burek, C.J., Daniel, P.T., Schulze-Osthoff, K., and Los, M. (2006). Apoptin-induced cell death is modulated by Bcl-2 family members and is Apaf-1dependent. Oncogene *25*, 2213-2222.

Coles, C., Condie, A., Chetty, U., Steel, C.M., Evans, H.J., and Prosser, J. (1992). p53 mutations in breast cancer. Cancer Res *52*, 5291-5298.

Cotter, T.G. (2009). Apoptosis and cancer: the genesis of a research field. Nat Rev Cancer *9*, 501-507.

Danen-van Oorschot, A.A.A.M., Zhang, Y.H., Leliveld, S.R., Rohn, J.L., Seelen, M.C.M.J., Bolk, M.W., van Zon, A., Erkeland, S.J., Abrahams, J.P., Mumberg, D., *et al.* (2003). Importance of nuclear localization of apoptin for tumor-specific induction of apoptosis. J Biol Chem *278*, 27729-27736.

DanenVanOorschot, A.A.A.M., Fischer, D.F., Grimbergen, J.M., Klein, B., Zhuang, S.M., Falkenburg, J.H.F., Backendorf, C., Quax, P.H.A., VanderEb, A.J., and Noteborn, M.H.M. (1997). Apoptin induces apoptosis in human transformed and malignant cells but not in normal cells. P Natl Acad Sci USA *94*, 5843-5847.

Dharap, S.S., and Minko, T. (2003). Targeted proapoptotic LHRH-BH3 peptide. Pharmaceut Res *20*, 889-896.

Dharap, S.S., Qiu, B., Williams, G.C., Sinko, P., Stein, S., and Minko, T. (2003). Molecular targeting of drug delivery systems to ovarian cancer by BH3 and LHRH peptides. J Control Release *91*, 61-73.

Dharap, S.S., Wang, Y., Chandna, P., Khandare, J.J., Qiu, B., Gunaseelan, S., Sinko, P.J., Stein, S., Farmanfarmaian, A., and Minko, T. (2005). Tumor-specific targeting of an anticancer drug delivery system by LHRH peptide. P Natl Acad Sci USA *102*, 12962-12967.

Edelstein, M.L., Abedi, M.R., and Wixon, J. (2007). Gene therapy clinical trials worldwide to 2007 - an update. J Gene Med *9*, 833-842.

Friedler, A., Hansson, L.O., Veprintsev, D.B., Freund, S.M.V., Rippin, T.M., Nikolova, P.V., Proctor, M.R., Rudiger, S., and Fersht, A.R. (2002). A peptide that binds and stabilizes p53 core domain: Chaperone strategy for rescue of oncogenic mutants. P Natl Acad Sci USA *99*, 937-942.

Gibbs, J.B. (2000). Mechanism-based target identification and drug discovery in cancer research. Science *287*, 1969-1973.

Gu, Z., Biswas, A., Zhao, M.X., and Tang, Y. (2011). Tailoring nanocarriers for intracellular protein delivery. Chem Soc Rev *40*, 3638-3655.

Gu, Z., Yan, M., Hu, B.L., Joo, K.I., Biswas, A., Huang, Y., Lu, Y.F., Wang, P., and Tang, Y. (2009). Protein Nanocapsule Weaved with Enzymatically Degradable Polymeric Network. Nano Lett *9*, 4533-4538.

Harris, N., Dutlow, C., Eidne, K., Dong, K.W., Roberts, J., and Millar, R. (1991). Gonadotropin-Releasing-Hormone Gene-Expression in Mda-Mb-231 and Zr-75-1 Breast-Carcinoma Cell-Lines. Cancer Research *51*, 2577-2581.

Issaeva, N., Bozko, P., Enge, M., Protopopova, M., Verhoef, L.G.G.C., Masucci, M., Pramanik, A., and Selivanova, G. (2004). Small molecule RITA binds to p53, blocks p53-HDM-2 interaction and activates p53 function in tumors. Nat Med *10*, 1321-1328.

Kamaly, N., Xiao, Z.Y., Valencia, P.M., Radovic-Moreno, A.F., and Farokhzad, O.C. (2012). Targeted polymeric therapeutic nanoparticles: design, development and clinical translation. Chem Soc Rev *41*, 2971-3010.

Koo, H., Lee, S., Na, J.H., Kim, S.H., Hahn, S.K., Choi, K., Kwon, I.C., Jeong, S.Y., and Kim, K. (2012). Bioorthogonal Copper-Free Click Chemistry In Vivo for Tumor-Targeted Delivery of Nanoparticles. Angew Chem Int Edit *51*, 11836-11840.

Lacroix, M., Toillon, R.A., and Leclercq, G. (2006). p53 and breast cancer, an update. Endocr Relat Cancer *13*, 293-325.
Leliveld, S.R., Zhang, Y.H., Rohn, J.L., Noteborn, M.H.M., and Abrahams, J.P. (2003). Apoptin induces tumor-specific apoptosis as a globular multimer. J Biol Chem *278*, 9042-9051.
Los, M., Panigrahi, S., Rashedi, I., Mandal, S., Stetefeld, J., Essmann, F., and Schulze-Osthoff, K. (2009). Apoptin, a tumor-selective killer. Bba-Mol Cell Res *1793*, 1335-1342.
Mbua, N.E., Guo, J., Wolfert, M.A., Steet, R., and Boons, G.J. (2011). Strain-promoted alkyne-azide cycloadditions (SPAAC) reveal new features of glycoconjugate biosynthesis. Chembiochem *12*, 1912-1921.
Meister, A., and Tate, S.S. (1976). Glutathione and related gamma-glutamyl compounds: biosynthesis and utilization. Annual review of biochemistry *45*, 559-604.
Murriel, C.L., and Dowdy, S.F. (2006). Influence of protein transduction domains on intracellular delivery of macromolecules. Expert Opin Drug Deliv *3*, 739-746.
Nagy, A., and Schally, A.V. (2005). Targeting of cytotoxic luteinizing hormone-releasing hormone analogs to breast, ovarian, endometrial, and prostate cancers. Biol Reprod *73*, 851-859.
Ning, X.H., Guo, J., Wolfert, M.A., and Boons, G.J. (2008). Visualizing metabolically labeled glycoconjugates of living cells by copper-free and fast huisgen cycloadditions. Angew Chem Int Edit *47*, 2253-2255.
Noteborn, M.H.M. (2009). Proteins selectively killing tumor cells. Eur J Pharmacol *625*, 165-173.
Okorokov, A.L., Sherman, M.B., Plisson, C., Grinkevich, V., Sigmundsson, K., Selivanova, G., Milner, J., and Orlova, E.V. (2006). The structure of p53 tumour suppressor protein reveals the basis for its functional plasticity. Embo J *25*, 5191-5200.
Peng, D.J., Sun, J., Wang, Y.Z., Tian, J., Zhang, Y.H., Noteborn, M.H.M., and Qu, S. (2007). Inhibition of hepatocarcinoma by systemic delivery of Apoptin gene via the hepatic asialoglycoprotein receptor. Cancer Gene Ther *14*, 66-73.
Pietersen, A.M., van der Eb, M.M., Rademaker, H.J., van den Wollenberg, D.J.M., Rabelink, M.J.W.E., Kuppen, P.J.K., van Dierendonck, J.H., van Ormondt, H., Masman, D., van de Velde, C.J.H.*, et al.* (1999). Specific tumor-cell killing with adenovirus vectors containing the apoptin gene. Gene Ther *6*, 882-892.
Reed, J.C. (2003). Apoptosis-targeted therapies for cancer. Cancer Cell *3*, 17-22.
Rohn, J.L., Zhang, Y.H., Aalbers, R.I.J.M., Otto, N., den Hertog, J., Henriquez, N.V., van de Velde, C.J.H., Kuppen, P.J.K., Mumberg, D., Donner, P.*, et al.* (2002). A tumor-specific kinase activity regulates the viral death protein apoptin. J Biol Chem *277*, 50820-50827.
Russo, A., Terrasi, M., Agnese, V., Santini, D., and Bazan, V. (2006). Apoptosis: a relevant tool for anticancer therapy. Ann Oncol *17*, Vii115-Vii123.
Saller, E., Tom, E., Brunori, M., Otter, M., Estreicher, A., Mack, D.H., and Iggo, R. (1999). Increased apoptosis induction by 121F mutant p53. Embo J *18*, 4424-4437.
Senzer, N., Nemunaitis, J., Nemunaitis, M., Lamont, J., Gore, M., Gabra, H., Eeles, R., Sodha, N., Lynch, F.J., Zumstein, L.A.*, et al.* (2007). p53 therapy in a patient with Li-Fraumeni syndrome. Mol Cancer Ther *6*, 1478-1482.
Shi, J.J., Votruba, A.R., Farokhzad, O.C., and Langer, R. (2010). Nanotechnology in Drug Delivery and Tissue Engineering: From Discovery to Applications. Nano Lett *10*, 3223-3230.
Sun, J., Yan, Y., Wang, X.T., Liu, X.W., Peng, D.J., Wang, M., Tian, J., Zong, Y.Q., Zhang, Y.H., Noteborn, M.H.M.*, et al.* (2009). PTD4-apoptin protein therapy inhibits tumor growth in vivo. Int J Cancer *124*, 2973-2981.
Tavassoli, M., Guelen, L., Paterson, H., Gaken, J., Meyers, M., and Farzaneh, F. (2004). Tumour specific induction of apoptosis by apoptin: Using DNA and protein. Cancer Gene Ther *11*, 856-856.
Tidow, H., Melero, R., Mylonas, E., Freund, S.M.V., Grossmann, J.G., Carazo, J.M., Svergun, D.I., Valle, M., and Fersht, A.R. (2007). Quaternary structures of tumor suppressor p53 and a specific p53-DNA complex. P Natl Acad Sci USA *104*, 12324-12329.
van der Eb, M.M., Pietersen, A.M., Speetjens, F.M., Kuppen, P.J.K., van de Velde, C.J.H., Noteborn, M.H.M., and Hoeben, R.C. (2002). Gene therapy with Apoptin induces regression of xenografted human hepatomas. Cancer Gene Ther *9*, 53-61.
Vassilev, L.T., Vu, B.T., Graves, B., Carvajal, D., Podlaski, F., Filipovic, Z., Kong, N., Kammlott, U., Lukacs, C., Klein, C.*, et al.* (2004). In vivo activation of the p53 pathway by small-molecule antagonists of MDM2. Science *303*, 844-848.
Welser, K., Perera, M.D.A., Aylott, J.W., and Chan, W.C. (2009). A facile method to clickable sensing polymeric nanoparticles. Chem Commun, 6601-6603.
Yan, M., Du, J., Gu, Z., Liang, M., Hu, Y., Zhang, W., Priceman, S., Wu, L., Zhou, Z.H., Liu, Z.*, et al.* (2010). A novel intracellular protein delivery platform based on single-protein nanocapsules. Nat Nanotechnol *5*, 48-53.
Zhao, M.X., Biswas, A., Hu, B.L., Joo, K.I., Wang, P., Gu, Z., and Tang, Y. (2011). Redox-responsive nanocapsules for intracellular protein delivery. Biomaterials *32*, 5223-5230.
Zhuang, S.M., Shvarts, A., Vanormondt, H., Jochemsen, A.G., Vandereb, A.J., and Noteborn, M.H.M. (1995). Apoptin, a Protein-Derived from Chicken Anemia Virus, Induces P53-Independent Apoptosis in Human Osteosarcoma Cells. Cancer Res *55*, 486-489.